ELSEVIER

Physica D 154 (2001) 259–286

PHYSICA D

www.elsevier.com/locate/physd

What symbolic dynamics do we get with a misplaced partition? On the validity of threshold crossings analysis of chaotic time-series

Erik M. Bollt [a,*], Theodore Stanford [b], Ying-Cheng Lai [c], Karol Życzkowski

[a] *Mathematics Department, 572 Holloway Road, US Naval Academy, Annapolis, MD 21402-5002, USA*
[b] *Department of Mathematical Sciences, New Mexico State University, Department 3MB, Las Cruces, NM 88003-8801, USA*
[c] *Departments of Mathematics, Electrical Engineering, and Physics, Center for Systems Science and Engineering Research, Arizona State University, Tempe, AZ 85287-1804, USA*
[d] *Centrum Fizyki Teoretycznej PAN, al. Lotników 32/46, 02-668 Warsaw, Poland*
[e] *Instytut Fizyki im. Smoluchowskiego, Uniwersytet Jagielloński, ul. Reymonta 4, 30-059 Kraków, Poland*

Received 8 August 2000; received in revised form 15 February 2001; accepted 16 February 2001

Communicated by C.K.R.T. Jones

Abstract

An increasingly popular method of encoding chaotic time-series from physical experiments is the so-called threshold crossings technique, where one simply replaces the real valued data with symbolic data of relative positions to an arbitrary partition at discrete times. The implication has been that this symbolic encoding describes the original dynamical system. On the other hand, the literature on generating partitions of non-hyperbolic dynamical systems has shown that a good partition is non-trivial to find. It is believed that the generating partition of non-uniformly hyperbolic dynamical system connects "primary tangencies", which are generally not simple lines as used by a threshold crossings. Therefore, we investigate consequences of using itineraries generated by a non-generating partition. We do most of our rigorous analysis using the tent map as a benchmark example, but show numerically that our results likely generalize. In summary, we find the misrepresentation of the dynamical system by "sample-path" symbolic dynamics of an arbitrary partition can be severe, including (sometimes extremely) diminished topological entropy, and a high degree of non-uniqueness. Interestingly, we find topological entropy as a function of misplacement to be devil's staircase-like, but surprisingly non-monotone.

PACS: 05.45.+b; 47.52.+j; 47.53.+n; 95.10.Fh

Keywords: Symbol dynamics; Topological entropy; Kneading theory; Devil's staircase

1. Introduction

Complicated evolution of a chaotic dynamical system is most easily understood in terms of a symbol dynamics representation, when a conjugating change of coordinates is available. Symbol dynamics and the Smale horseshoe

* Corresponding author.
E-mail addresses: bollt@nadn.navy.mil (E.M. Bollt), stanford@nadn.navy.mil (T. Stanford), yclai@chaos1.la.asu.edu (Y.-C. Lai), karol@tatry.if.uj.edu.pl (K. Życzkowski).

0167-2789/01/$ – see front matter
PII: S0167-2789(01)00242-1

[1] ushered a revolution in describing and defining long term evolution of chaotic dynamical systems. Ideally, a "generating" partition is used to give each point in the phase space a unique itinerary sequence recorded in the symbol space. However, generating partitions are not easily obtained in practice. The concept of Markov partitions for hyperbolic dynamical systems, including Anosov diffeomorphisms [2] and Axiom A systems is well defined. Likewise, Markov maps are well defined for maps of the interval [3], as are generating partitions [4]. However, in the general cases of planar non-uniformly hyperbolic maps [5] or higher than two-dimensional maps [6], a well-defined generating partition is highly non-trivial. There are special case studies suggesting a conjecture for the generating partitions for certain non-uniformly hyperbolic planar maps, including the Hénon map [7], the standard map [8,36], and billiards maps [9,37]; the arguments of validity are convincing, but heuristic.

In this work, we take a different approach. We ask, what are the consequences of a misplaced partition? The generating partition is defined as a partition for which the topological entropy achieves its supremum. Thus the entropy of a symbolic sequence generated by a misplaced partition cannot be larger than the topological entropy of the dynamical system. In general, the misplacement of the partition leads to *diminishing* of the computed entropy of the system.

Suppose we choose an arbitrary topological partition of the phase space. Then the orbit of each initial condition will have *some* infinite itinerary through this partition under the action of the map. To what degree is the sample-path dynamics of the map not represented by this "misplaced", symbol dynamics? Considering the tent map, for which the generating partition and the symbolic dynamics are well known, allows us to compare consequences of deliberate misplacement. In brief, due to misplacing the partition, some (often uncountably many) state points which formerly had distinguished symbolic itineraries, become indistinguishable with respect to their misplaced partition itineraries. We see these "identifications" and hence diminished subshift reflected in a topological entropy versus misplacement function which is devil's staircase-like, but surprisingly non-monotone. To make the loss of representation obvious, consider the situation in which there is a conjugacy to a fullshift on several symbols (the standard map, for example has a subshift on seven symbols [8,36]), but an arbitrary threshold crossing partition of say two symbols must necessarily lead to a diminished representation. Even if enough partition-elements/symbols are chosen it is likely that the arbitrary partition does not give the maximal entropy measure, and hence there will be a diminished representation. In this paper, we study specifically the nature of such loss of representation.

Our motivation to pursue this problem is physically practical. While a grammatical representation in symbol space is widely considered a simplifying generalization of a complicated dynamical system, a general method to find a generating partition is not known. Nonetheless, arbitrary partitions have already (sometimes unwittingly) become popular in the physical literature [10–12], due to the fact that generating partitions are so difficult to find. One can find non-generating partition studies in the literature in [11] studying an internal combustion engine [10] evaluating risk of death in patients with coronary disease, and in cognitive psychology in the study of movement control [12]. "Threshold crossings" is a popular technique for experimental time-series which essentially chooses some (arbitrary) partition, and then one studies the resulting sample-path symbolic dynamics relative to this partition in proxy of a more direct analysis, such as time-delay embedding (see [13] and references therein). We consider our studies of the symbol dynamics relative to an arbitrary partition as a good proving ground to shed light on the severe problems which likely arise with such a replacement. Only in a controlled benchmark setting where we can compare the misplaced symbolic dynamics to the true symbolic dynamics can we draw (often rigorous) conclusions of such practices. In brief, we find that well placing a partition is crucial even for making rough generalizations, and therefore we have serious doubts concerning the practice of threshold crossings analysis.

In terms of a physical model, the idea behind threshold crossings is natural and fundamental. In science, after collecting data one wishes to interpret these data. This may mean associating adjectives, i.e., "hot" versus "cold", "full" versus "empty", "big", "medium", or "small", etc. In such cases, it is necessary to partition these states. On the other hand, one may wish to retain pure measurements. But no physical measurements are truly real numbers.

Accuracy thresholds implies a finite number of significant figures, and hence there are necessarily a finite number of partitioned states for each measured variable, each of which has a threshold. The fundamental question we ask in this paper is this: *does an arbitrary coarse-grained partitioning of dynamical data, which is not generating, in some sense reflect the dynamical system*?

Consider, for example a time-series describing temperature measured at some locale everyday at noon. We presume that the data is generated by some underlying dynamical process. Say we call a temperature cold (or "0" for that matter) every time the noon time temperature is $\leq p^{\circ}$C. Call the temperature hot (or "1") otherwise. We ask how such a replacement reflects the dynamical process. Certainly, a well chosen partition is important, as exemplified by choosing $p = -100^{\circ}$C (which of course never happens in the authors' home towns), and therefore, the symbolic stream is all "1's". Likewise, $p = 100^{\circ}$C would give all "0's", which corresponds to the entropy equal to zero. Just how the grammar of the corresponding symbolic dynamics varies with changing threshold partitions $-100^{\circ}\text{C} < p < 100^{\circ}\text{C}$ is therefore a practical problem with surprising complexity. Furthermore, we have good reason to believe that, generically, no threshold crossing partition symbolic dynamics will reflect the dynamical process which generated the data being analyzed. In fact, the misrepresentation by even the optimal threshold crossing can be severe, bringing such practice into question. Not losing sight of our original physical motivation, we believe, but cannot prove, that most of the essential problems of a misplaced partition are typical and displayed even by real world data sets. Laboratory data results is presented in Section 9.

The main implication of our results is that the threshold-crossing technique typically yields misleading conclusions about the dynamics generating the data, and therefore one should be extremely cautious when attempting to understand the underlying system from a misrepresented symbolic dynamics. We have written a brief presentation of some of these results [14].

In this work, we study the consequences on the "sample-path" symbolic dynamics due to an exactly misplaced partition, of a deterministic (noise-less) dynamical system. We consider this to be a physically relevant problem statement, as outlined above regarding the difficulties of finding generating partitions in physically relevant dynamical systems, and considering the current popularity of the threshold-crossing technique. Another complementary problem, which we have not considered in this work, would be to consider the consequences on the sample-path symbolic dynamics due to a stochastic dynamical system, say of the form of a deterministic map plus a small noise perturbation at each step of the form $x_{n+1} = f(x_n) + \epsilon\xi_n$, where ξ_n is a identically distributed independent random variable. A previous study on the role of noise on the symbolic dynamics, due to Crutchfield and Packard [15,38] concludes that entropy increases according to a power law with noise volume, and that fine structures of invariant measure blur at the noise threshold, see also [16]. Similar topological entropy figures to ours have appeared previously [15,17,38], but our combinatorial and topological explanation of the phenomenon and application is new, and leads to a deep understanding of the phenomenon. Our work is rather complementary to this previous research, since we studied the role of an exactly misplaced partition, whereby stochastic operator techniques allow study of the blurring effects of noise [15,16,38].

We give an overview technical summary of the content in this paper in Section 10, which could equally serve as a preview summary for those who wish to read such a table of contents paragraph now.

2. The tent map and partitions

We study a simplified setting in which the true Markov partition is well known, and many calculations may be performed in closed form. Thus, we are motived to choose the tent map, $f : [0, 1] \to [0, 1]$,

$$x_{n+1} = f(x_n) = 1 - 2|x_n - \tfrac{1}{2}|. \tag{1}$$

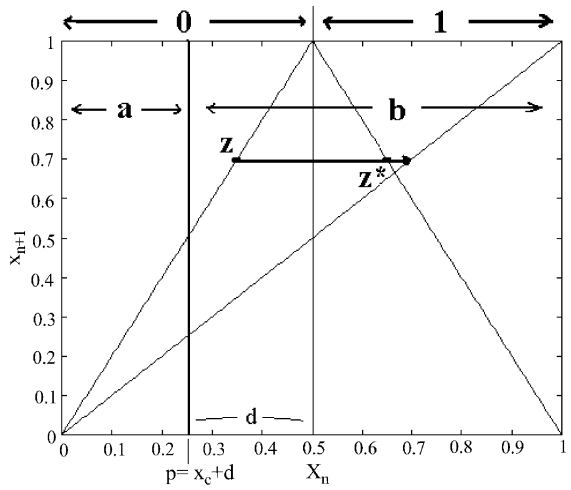

Fig. 1. Tent map, and misplaced partition at $p = x_c + d$.

The tent map is well known [3,18,19] to have a Markov partition at $x_c = \frac{1}{2}$, which corresponds to the topological entropy $h_t = \ln 2$. The dynamics of $f|_{[0,1]}$ are semi-conjugate to the Bernoulli full 2-shift $s|_{\Sigma_2}$ by the surjection $h : [0, 1] \to \Sigma_2$ which gives a symbolic itinerary $\sigma = \sigma_0 \cdot \sigma_1\sigma_2 \cdots$ for each $x \in [0, 1]$,

$$\sigma_i(x) = \begin{cases} 0 & \text{if } f^i(x) < x_c, \quad i \geq 0, \\ 1 & \text{else}, \quad i \geq 0, \end{cases} \tag{2}$$

where we take $\Sigma_2^{\{0,1\}}$ to be the semi-infinite fullshift on two symbols $\{0, 1\}$. In fact, h is "almost" a conjugacy [1] [20]. We can consider gradually deforming the symbol dynamics of itineraries relative to $d \in [-\frac{1}{2}, \frac{1}{2}]$, a misplacement parameter. Itineraries relative to the misplaced partition

$$p = x_c + d, \tag{3}$$

are defined for each initial condition $x_0 \in [0, 1]$ by symbols "a" and "b",

$$\varphi_i(x) = \begin{cases} a & \text{if } f^i(x) < p, \quad i \geq 0, \\ b & \text{else}, \quad i \geq 0, \end{cases} \tag{4}$$

see Fig. 1. We expect a subshift of $\Sigma_2^{\{a,b\}}$. In our notation convention, $\sigma(x)$ denotes the infinite $\{0, 1\}$-itinerary of x, $\sigma_i(x) = 0$ or 1 denotes the position of $f^i(x)$ relative to $x_c = \frac{1}{2}$, and likewise $\varphi(x)$ gives a or b symbolic representation of the orbit relative to the misplaced partition p. Where the base point is obvious, for convenience we suppress the full notation, denoting $\sigma_i \equiv \sigma_i(x)$ or $\varphi_i \equiv \varphi_i(x)$.

[1] The relationship between the tent map and the symbol dynamics is only a semi-conjugacy, but there is almost a full conjugacy. Specifically, a totally disconnected set Σ_2 cannot be mapped continuously to an interval [0,1], but standard fix is analogous to the familiar repeating decimal identifications problem of defining decimal expansions for the real line (e.g., $0.4 \equiv 0.3999\ldots$. One must "close the gaps", of the Cantor set by identifying the symbolic itineraries of opposite open sides of the non-hyperbolic point x_c, and its pre-images. The problem occurs on only a countable set of points, the pre-images of the symbol partition, $\bigcup_{i=0}^{\infty} f^{-i}(c)$. The tent map is almost everywhere two-to-one, except at these points, and the fullshift map is everywhere two-to-one. There is ambiguity between $0100\cdots$ and $11000\cdots$, for the "correct" symbol representation of the point $c = \frac{1}{2}$. However, there is a conjugacy between the logistic map f_4, and the subshift Σ' consisting of the fullshift Σ in which all symbol sequences of the form $\sigma_0 \cdot \sigma_1 \cdots \sigma_k 01000\cdots$ (a pre-iterate of $01000\cdots$) are identified with $\sigma_0 \cdot \sigma_1 \cdots \sigma_k 11000\cdots$ [20].

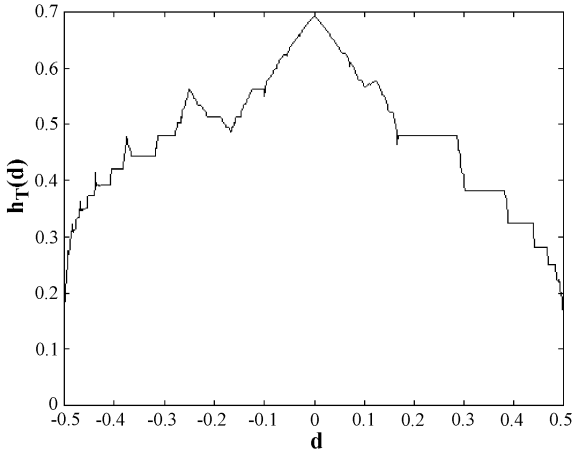

Fig. 2. Direct approximation of topological entropy versus displacement of partition, $h_T(d)$, for the tent map.

Amongst many interesting consequences, we find that typically, a given symbolic itinerary relative to the misplaced partition may correspond to infinitely many state points x_0. Furthermore, we find that the partition dependent entropy of the symbols sequence, $h_T(d)$, is a devil's staircase-like function of the displacement, d, but surprisingly non-monotone, see Figs. 2 and 6.

3. Numerically sampled *a*; *b* words, and topological entropy

We begin by observing $a; b$ itineraries and then approximate the topological entropy of observed orbits, relative to a misplaced partition. Given almost any initial condition, x_0, its orbit under the tent map $f(x)$ is dense in the interval [0, 1]. Choosing such an initial condition, and orbit segment $\{f^i(x_0)\}_{i=0}^N$, and given a specific partition p, we generate an $a; b$ itinerary, $\varphi_0 \cdot \varphi_1 \cdots \varphi_N$.

We approximate the topological entropy of $\Sigma_2^{\{a,b\}}(d)$ by the formula [21]

$$h_T(s|\Sigma_2^{\{a,b\}}(d)) = \limsup_{n\to\infty} \frac{\log(w_n)}{n}, \tag{5}$$

where w_n is the number of $a; b$ words of length n, which occur as an n-bit block for some $\varphi \in \Sigma_2^{\{a,b\}}(d)$. Note that simply considering possible permutations bounds $w_n \le 2^n$. The approximation is obtained by considering this lim sup as describing the exponential growth rate with n, of the allowable words of length n, and then doing so for a long, but finite list. The computer algorithm is as follows: choose $p = d + x_c$, choose N large, and choose almost any x_0 and generate $\{f^i(x_0)\}_{i=0}^N$ and then $\varphi_0 \cdot \varphi_1 \cdots \varphi_N$. Choose a large M, and for each $m \le M$, simply count the observed w_m, which is expected to be slightly less than maximal for large m, since our computer generated test orbit is finite. Then we fit a line to w_m versus m on a log scale, and the slope is taken to approximate topological entropy.

Choosing a grid of misplacements, $d \in [0, 1]$, we plot $h_T(d)$ in Fig. 2.

Remark 3.1. Three points can be verified immediately. For $d = 0$, $\Sigma_2^{\{a,b\}}(0)$ is the full 2-shift, and we observe $h_T(0) \approx \log(2)$ as expected. For $d = -\frac{1}{2}$, it is obvious that the grammar forbids the letter a, and therefore $\Sigma_2^{\{a,b\}}(-\frac{1}{2})$ consists of the single point $\varphi = b \cdot b\bar{b}$, and likewise $\Sigma_2^{\{a,b\}}(\frac{1}{2})$ consists of the single point $\varphi = a \cdot a\bar{a}$. Therefore, $h_T(-\frac{1}{2}) = h_T(\frac{1}{2}) = 0$.

Remark 3.2. Due to the two-to-one nature of the tent map, placing the partition at any $d \neq 0$ causes two points $x, \tilde{x} \in (x_c - |d|, x_c + |d|)$, which are symmetrically placed relative to x_c (see Fig. 1) to have the same future orbit *and* the same first bit starting position relative to p. Hence, they are indistinguishable. Such a loss in separate words might incorrectly lead us to conclude that $h_T(d)$ should be monotone decreasing such as was found in a tent-gap map [22,23,39]. Likewise, considering $(x_c - |d|, x_c + |d|)$ as a primary identification interval, one can show that any two points symmetrically located in a pre-image of the interval, a pre-image which does not intersect the primary interval, are also symbolically identical. In Section 9, we discuss ambiguities due to non-generating partitions.

4. A mechanism for non-monotonicity: relabeling a directed graph

Consider the case that the partition is misplaced at a position d whose value is a dyadic rational number

$$d = \frac{q}{r} = \frac{q}{2^n} \quad \text{for } q, r, n \in \mathbf{Z}^+, \quad d \in [0, 1]. \tag{6}$$

The fullshift $\Sigma_2^{\{0,1\}}$ is naturally presented in terms of a directed graph describing the 2^n, n-bit, words of 0's and 1's. In Fig. 3, we show the case $n = 4$; the $2^4 = 16$, 4-bit words are arranged left to right in this graph, by the Gray-code order in which one finds symbol sequences ordered monotone to the unit interval, according to the kneading theory [20,24]. For $n = 4$-bits, the $\prec$ order is $0000 \prec 0001 \prec 0010 \prec 0110 \prec \cdots \prec 1011 \prec 1001 \prec 1000$. Furthermore, we have deliberately made a hump-like pattern to the graph to remind us of the one-hump tent map, and the edges of the graph follow the tent map/Bernoulli shift map.

A *sophic shift* X is a shift space generated by all possible walks through a labeled graph $\mathcal{G} = (G, L)$ [25], where each edge carries a label indexing L, and a particular element of X is defined by the labels of the set of edges followed during a particular infinite walk.

A sophic shift is defined to be *right-resolving* if each vertex has all of its exiting edges labeled uniquely. For example, Fig. 3 is a right-resolving (but not minimal) presentation of a sophic shift which is conjugate to the full 2-shift.

Dyadic, Eq. (6), misplacements of the partition Equation (3) are prominent in our work due to the following observation. If the misplacement occurs at a dyadic d, then the partition of the tent map can be described in symbol

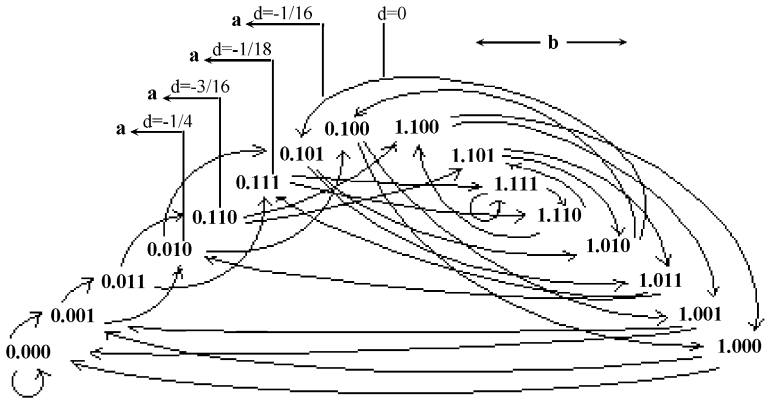

Fig. 3. Full two-shift, presented as the action of the Bernoulli shift map on all 4-bit words, and Gray-code ordered left to right, according to a one-hump map kneading. Some dyadic misplacements are shown according to Eq. (6) with denominator $n = 4$. See Example 4.3, for the non-monotonicity mechanism, whereby the word *abbba* is *temporarily* lost as d decreases.

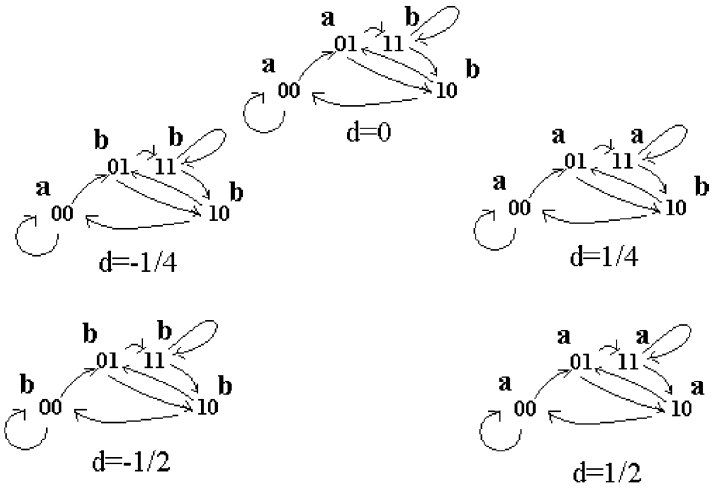

Fig. 4. All possible dyadic misplacements, according to Eq. (6) with denominator $n = 2$. a; b relabelings are shown for each d.

space by relabeling the set of edges of an appropriate de Broijn graph $\mathcal{G} = (G, L)$ [25] presentation of the fullshift. This de Broijn graph presentation is a graph showing all 2^m-bit words, and transitions, for $m \geq n$ if the denominator in Eq. (6) is 2^n. Misplacing the partition to any such d is equivalent to relabeling the set of edges in this appropriate presenting graph, to be either a or b, according to the Gray-code order (i.e., the kneading order). If $d \preceq v_i$, where $v_i, i = 1, \ldots, 2^n$ is the ith n-bit word labeling a vertex, then all edges pointed *into* that vertex are relabeled as an a, and otherwise as a b. This respects Eq. (4). Such a relabeling can be considered to be a factor code ϕ_d, projecting $\phi_d : \Sigma_2^{\{0,1\}} \to \Sigma_2^{\{a,b\}}(d)$ surjectively, where $\Sigma_2^{\{a,b\}}(d)$ denotes the subshift which is conjugate to the sophic shift defined by the just defined "appropriate", but relabeled graph (G, L). In other words, the choice of dyadic d is purely a matter of convenience for clear presentation and calculation. [2]

These relabeled graphs each define a new subshift, by considering all walks through the graph, and all resulting infinite sequences of a's and b's. A subshift is of finite type if it has a finite length longest minimal forbidden word. The degree of the grammar (longest minimal forbidden word) of these new (relabeled) subshifts is not immediately obvious, nor indeed is it even true that these new subshifts are even of finite-type. The techniques developed in the next section address this issue. For now, we consider examples.

Example 4.1. If $d = \pm\frac{1}{2}$, then all paths are labeled either $b\bar{b}(+)$ or $a\bar{a}(-)$. Hence the grammar forbids either $a(+)$ or $b(-)$, and $h_T(\pm\frac{1}{2}) = 0$ agrees with Fig. 2. This example possibly leads to a false intuition that as $|d|$ increases, the grammar should become more restrictive, as paths become relabeled, and $h_T(d)$ should decrease monotonically. We see in Fig. 2 that this is false. Example 4.3, and Remark 4.1, describe the mechanism behind the mistake.

Example 4.2. Consider $n = 2$, and $d = -\frac{1}{4}$. This is an a; b relabeling as shown in Fig. 4. The reader can check that the 3-bit word *aba* is forbidden in the sophic shift, because starting from 00, the only vertex labeled a, follow

[2] The choice of d dyadic is merely a matter of convenience. Many of our calculations, which depend on relabeling graphic presentations of sophic shifts are possible, though less conveniently so, for other rational values of d. Also, we have recently proven a result whose proof we will report elsewhere: a certain family of the flat spots of the function $h_T(d)$ exists for a corresponding family of open intervals. Thus, the devil's staircase is not just a result of the dyadic points chose. Furthermore, at least for the family of open sets mentioned, $h_T(d)$ is a continuous, and constant function.

vertices labeled $\overbrace{00}^{a} \to \overbrace{01}^{b} \to \begin{matrix}\overbrace{10}^{b}\\ \text{-or-}\\ \overbrace{11}^{b}\end{matrix}$. In Section 6, we give an algorithm which shows that *aba* is in fact the minimal forbidden word, and which automatically finds the grammar for other misplacements.

The next example shows a mechanism which gives the non-monotonic $h_T(d)$ function.

Example 4.3. We show that when $n = 4$, and $d = -\frac{1}{8}$, the relabeled word *abbba* is allowed, and is generated by the path $\overbrace{0111}^{a} \to \overbrace{1110}^{b} \to \overbrace{1100}^{b} \to \overbrace{1001}^{b} \to \overbrace{0010}^{a}$, and it can be checked that this is the only such labeled path through the graph, see Fig. 3. Now if the partition is further misplaced to $d = -\frac{3}{16}$, then that path gains the new identity *bbbba*, since $\overbrace{0111}^{b} \to \overbrace{1110}^{b} \to \overbrace{1100}^{b} \to \overbrace{1001}^{b} \to \overbrace{0010}^{a}$ by relabeling of vertex 0111 from *a* to *b*. It can be checked that this was the only path which gave *abbba*, when $d = -\frac{1}{8}$, and so when $d = -\frac{3}{16}$, this *abbba* can label no other paths, and the word becomes forbidden. In Appendix A, we verify this statement by checking all possible cases. However, the word *abbba* identifies a new path, when the partition is further misplacement to $d = -\frac{1}{4}$: $\overbrace{0011}^{a} \to \overbrace{0110}^{b} \to \overbrace{1100}^{b} \to \overbrace{1000}^{b} \to \overbrace{0000}^{a}$ was formerly named *aabba*. We observe that $d = -\frac{3}{8}$ appears to be a local maximum of $h_T(d)$ in Figs. 2 and 6.

Remark 4.1. Example 4.3 displays a mechanism which dispels the bad intuition, outlined in Example 4.1 that $h_T(d)$ should be monotone with $|d|$. We summarize the mechanism: (1) a path (or several paths) paths is labeled by an n-bit a; b word w_n when $d = d_1$, (2) when $d = d_2$, where $|d_2| > |d_1|$, and $d_1 d_2 > 0$, then that path is relabeled (and never carries the label w_n for any d beyond d_2) and w_n is not realized by any other path for $d = d_2$, (3) when $d = d_3$, the further change in misplacement causes another path to assume the label w_n, thus possibly increasing the set of allowed a; b words and the entropy.

5. A right-resolving presentation of the misplacement sophic shift

In this section, we give an algorithm which generates a right-resolving presentation of the sophic shift generated by a dyadic misplacement d. Our construction is a convenient way to describe the subset construction found in [25]. Using this algorithm, we can make further statements concerning the generated subshift. In particular, we will calculate topological entropy by the spectral radius calculation based on Perron–Frobenius theory.

First, we recall some important theorems [25].

Theorem 5.1 (Lind and Marcus [25], 4.3.3(1) and 4.4.4). *Let X be a sophic shift, and $\mathcal{G} = (G, L)$ be a right-resolving presentation of X, then $h_T(X) = \ln \rho(A(G))$, where $\rho(A(G))$ is the spectral radius (i.e. the modulus of the largest eigenvalue) of the transition matrix A corresponding to G.*

Since the sophic shifts generated by a misplaced partition, Eq. (4), are generally not right-resolving, the following existence theorem is important.

Theorem 5.2 (Lind and Marcus [25], 3.3.2). *Every sophic shift has a right-resolving presentation.*

We now describe the following constructive algorithm which allows us to actually generate a right-resolving presentation of a graph presented directly from Eq. (4).

5.1. Algorithmic construction of right-resolving presentation

Let $d = q/2^n$ be dyadic. Then the (misplaced) sophic shift $\Sigma_2^{\{a,b\}}(d)$ may be presented by relabeling the $N = 2^n$ vertices of the de Broijn graph presentation of the fullshift $\Sigma_2^{\{0,1\}}$ (i.e., see Fig. 3 for the $n = 4$ de Broijn graph) according to Eq. (4). Define the graph which generates $X_{\mathcal{G}} \equiv \Sigma_2^{\{a,b\}}(d)$ to be $\mathcal{G} = (G, L)$. $X_{\mathcal{G}}$ is sophic by construction, but generally not right-resolving.

Index each of the N vertices of G, G_i, $i = 1, 2, \ldots, 2^n$ and define a new set of vertices $H = \{H_j\}_{j=1}^{2^N}$. Let each H_j define specific and unique on/off (toggle-switch like) states for each vertex. For convenience, label each H_j by NX's and O's, which left to right each give an on/off state for each G_i, see example below. In this notation, suppose only G_i is to be "turned on", then $H_j = 00\cdots0X0\cdots0$ has an X (on) only in the ith position. Considering all on/off states of $\{G_i\}_{i=1}^N$ requires 2^N vertices H_j.

Now, we must define edges E to go with the vertices H. Each H_j labels on/off positions of N, G_i vertices of G. Consider *all of those vertices* G_k which can follow each of these G_i *such that each* G_k *has the label* "a", to be "turned on", and all other G_k to be "turned off". If none of these G_i transition to an a label G_k, then no edge will be defined. Thus, for each non-empty transition, a vertex H_l is defined to follow H_j with an a. Similarly, define "b" edges from H_j. Hence, we construct a graph $\mathcal{H} = (H, E)$ which generates a sophic shift $X_{\mathcal{H}}$. The following propositions can be easily shown to follow by our constructions.

Proposition 5.1. *$X_{\mathcal{H}}$ is conjugate to $\Sigma_2^{\{a,b\}}(d)$, and hence $h_{\mathrm{T}}(X_{\mathcal{H}}) = h_{\mathrm{T}}(\Sigma_2^{\{a,b\}}(d))$.*

Proposition 5.2. *$\mathcal{H} = (H, E)$ is a right-resolving presentation of $\Sigma_2^{\{a,b\}}(d)$.*

Example 5.1. Let $n = 2$ and therefore $N = 4$, and let $d = -\frac{1}{4}$, see Fig. 4. The de Broijn graph presentation of $\Sigma_2^{\{a,b\}}(-\frac{1}{4})$ has vertices labeled 00, 01, 11, and 10. Define $H = \{XOOO, OXOO, OOXO, OOOX, XXOO, \ldots, XXXX\}$ to have 16 elements where we interpret for example $XOOO$ to mean that only 00 is "turned-on", and $XXOO$ means that 00 and 01 are on, see Fig. 5 for the complete construction of $\mathcal{H} = (H, E)$.

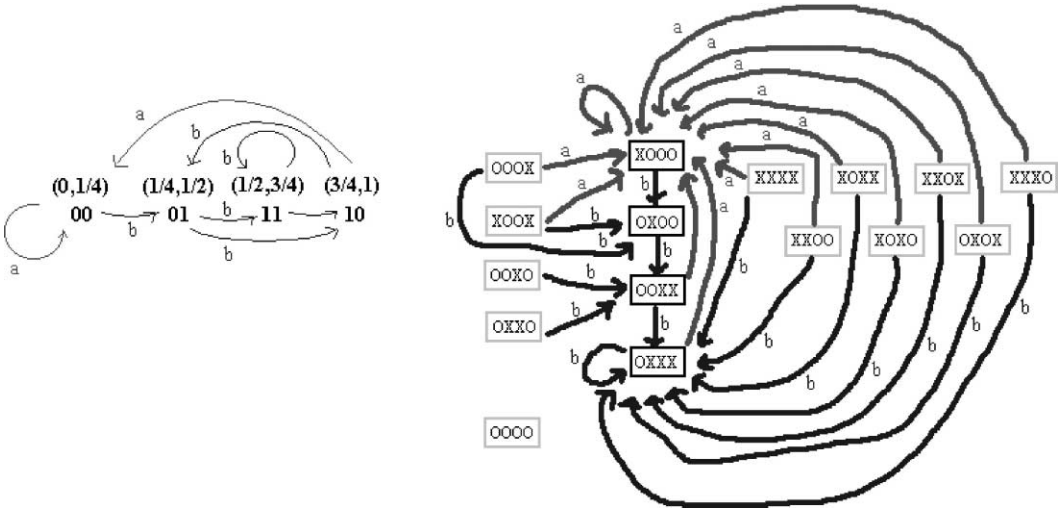

Fig. 5. Construction of a right-resolving presentation of $\Sigma_2^{\{a,b\}}(-\frac{1}{4})$.

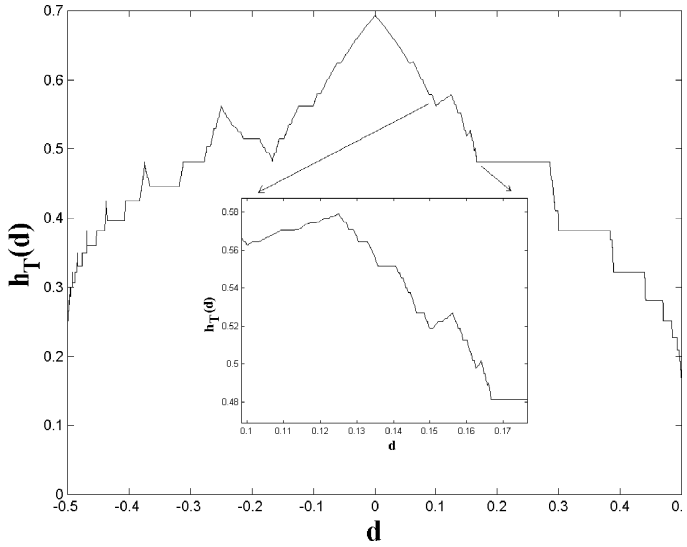

Fig. 6. Exact calculation of $h_T(\Sigma_2^{\{a,b\}}(d))$. Compare with Fig. 2.

This algorithm is readily automated as a computer program which will "exactly" compute $h_T(\Sigma_2^{\{a,b\}}(d))$ for a sequence of $d = q/2^n$, $q = 0, 1, \ldots, 2^n$ for fixed n. Since $\mathcal{H}$ has 2^{2^n} vertices, in practice it is computationally expensive to fully follow the above construction for misplacements with large denominators. Experimentally, however, we have found that $\mathcal{H}$ typically has a small irreducible subcomponent which, because of the irreducibility of the tent map, generates the same symbol dynamics as all of $\mathcal{H}$ (see Fig. 5 for example). In particular, we have found that an efficient algorithm to calculate the entropy is to use the subgraph of $\mathcal{H}$ consisting of all vertices which follow the vertex $XXX\cdots X$, with every vertex of the de Broijn graph turned on. We have successfully been able to generate exact graphs for $d = p/2^n$ for n as large as $n = 16$. Following the algorithm described in this section, we consider Fig. 6 to be "essentially" exact, since the directed graphs are exact. Calculating eigenvalues for such large matrices must be numerical, but the numerical analysis of controlling such errors is standard and precise. Furthermore, for small n, $\rho(C(H))$ can be found exactly by computer assisted algebra.

Note the similarity between Figs. 2 and 6, which were derived by two very different methods. Please also note the finer structures which appear in Fig. 6, which apparently appear on all scales. There are devil's staircase-like steps and flat spots, but also non-monotonicity.

6. Determination of forbidden words

The right-resolving construction in the previous section is useful for entropy calculations, but does not yield the grammar of a particular misplaced subshift in the form of a list of forbidden words. In this section, we develop an algebra of multiplying appropriate matrices to determine the complete list of forbidden words of a given misplaced subshift $\Sigma_2^{\{a,b\}}(d)$ for certain d, including dyadic d.

We remark that even given a sophic shift, with its generating graph $\mathcal{G} = (G, L)$, listing forbidden words is a non-trivial task. It is not even true that a finite graph gives a subshift of finite type. Consider the following simple example called the "odd shift" (related to the so-called "even shift" [25]), which affirms this fact.

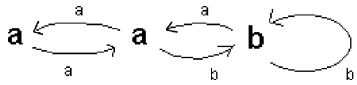

Fig. 7. The odd shift has no even runs of a.

Example 6.1 (Odd shift). Let $\Sigma_2^{\{a,b\}'} \subset \Sigma_2^{\{a,b\}}$ be a subshift defined by all infinite sequences of a and b, such that no words (blocks) w have a run of a's of even length. Therefore, the list of minimal forbidden words is $\{baab, baaaab, baaaaaab, \ldots, b(a)^{2m}b, \ldots\}$ is obviously infinite, and hence the odd shift is of infinite type. Nonetheless, it has the simple finite generating graph depicted in Fig. 7.

Now we shall construct a finite semigroup, which allows us to determine the list of minimal forbidden words of any sophic shift. The semigroup is constructed by modifying the transition matrix C of underlying graph $\mathcal{G} = (G, L)$ of the sophic shift. For ease of presentation, we describe the construction based on only two symbols, but it is easily generalized.

Let $\mathcal{G} = (G, L)$ have all vertices labeled either a or b. Let C be the transition matrix defined as

$$C_{i,j} = \begin{cases} 1 & \text{if there is an edge between vertices } G_i \text{ to } G_j, \\ 0 & \text{otherwise.} \end{cases} \tag{7}$$

Hence, C makes no regard for the "color" of the transition. Now define A to be the part of C which carries transitions labeled a; let

$$A_{i,j} = \begin{cases} 1 & \text{if } C_{i,j} = 1 \text{ and } G_j \text{ is labeled } a, \\ 0 & \text{otherwise.} \end{cases} \tag{8}$$

Let B be defined similarly to carry only the b transitions. Note that $C = A + B$.

Now we can state a proposition concerning characterization of the grammar which follows directly from the construction of the matrices A, B and D. Thus we may reduce the search for forbidden words to matrix multiplication, which is simple for numerical investigation.

Proposition 6.1 (Grammar characterization by matrices). *Let $D_i = A$ or B be the above labeled transition matrices of the sophic shift $\Sigma_2^{\{a,b\}}$ generated by $\mathcal{G} = (G, L)$. Let $d_i = a$ or b define symbols. A word $w = d_1 d_2, \ldots, d_n$ is forbidden, not appearing as a block any $\sigma \in \Sigma_2^{\{a,b\}}$ iff the correspondingly labeled matrix product satisfies $D_n \cdot D_{n-1} \cdots D_1 = D_n \prod_{i=1}^{n-1} D_i = \mathbf{0}$.*

Remark 6.1. A key observation is that our 0; 1 arithmetic of matrix multiplication defined as follows generates a finite set of matrices which is closed under the multiplication. We define the *semigroup* to be the closed set of matrices generated by products of (typically two, A and B) transition matrices. Now we define semigroup 0; 1 matrix multiplication. Every element of the semigroup is a matrix of 0 and 1 entries. Suppose X and Y are matrix elements of the semigroup, then each i, jth entry of the standard matrix product $X \cdot Y$ which is >1 is set to be 1. For example, suppose that $X = \begin{pmatrix} 1 & 1 \\ 0 & 1 \end{pmatrix}$ and $Y = \begin{pmatrix} 0 & 1 \\ 1 & 1 \end{pmatrix}$ are two elements from some semigroup. Then since standard matrix multiplication gives $\begin{pmatrix} 1 & 1 \\ 0 & 1 \end{pmatrix} \cdot \begin{pmatrix} 0 & 1 \\ 1 & 1 \end{pmatrix} = \begin{pmatrix} 1 & 2 \\ 1 & 1 \end{pmatrix}$, we define $X \cdot Y = \begin{pmatrix} 1 & 1 \\ 1 & 1 \end{pmatrix}$. Since the number of $n \times n0$; 1 matrices is finite, it follows immediately that *a semigroup generated by finite matrices is finite.*

This is crucial for what follows, as it provides that our algorithms to determine the grammar of a sophic shift have finite termination.

Example 6.2 (Odd shift continued). The directed graph in Fig. 7 has the transition matrix

$$C = \begin{pmatrix} 0 & 1 & 0 \\ 1 & 0 & 1 \\ 0 & 1 & 1 \end{pmatrix}, \tag{9}$$

and considering each only those transitions carrying the label a or b gives

$$A = \begin{pmatrix} 0 & 0 & 0 \\ 0 & 0 & 1 \\ 0 & 0 & 1 \end{pmatrix}, \quad \text{and likewise} \quad B = \begin{pmatrix} 0 & 1 & 0 \\ 1 & 0 & 0 \\ 0 & 1 & 0 \end{pmatrix}. \tag{10}$$

Now we can generate all possible sets of words by starting with a and b since both A and B are non-zero. Then we right multiply by all possible (matrix) words of length 1, then 2, etc. One might expect that this will create an infinite list, but certain matrix identities appear. For example, check that $B \cdot B = B$ and therefore any run of b's is allowed. We now list the identities, and forbidden words we have found

$$\text{Identities :} \quad B \cdot B = B, \quad A \cdot A \cdot A = A, \quad B \cdot A \cdot B = B, \quad B \cdot A \cdot B \cdot A = B \cdot A, \quad A \cdot B \cdot A \cdot B = A \cdot B, \tag{11}$$

$$\text{Forbidden :} \quad B \cdot A \cdot A \cdot B = \mathbf{0}. \tag{12}$$

Observe that $B \cdot A \cdot A \cdot B = \mathbf{0}$ means that no two a's in a row are allowed, and together with the identity $A \cdot A \cdot A = A$ implies that no even runs of a are allowed which recovers the definition of the odd shift, $\Sigma_2^{\{a,b\}'}$. Following an exhaustive search for new words of ever longer length, and using the identities of longer length as they appear gives a list of allowed words

$$\text{Allowed matrix words :} \quad A, \quad B, \quad A \cdot A, \quad A \cdot B, \quad B \cdot A, \quad A \cdot A \cdot B, \quad A \cdot B \cdot A, \quad B \cdot A \cdot A, \quad A \cdot A \cdot B \cdot A, \quad A \cdot B \cdot A \cdot A, \quad A \cdot A \cdot B \cdot A \cdot A. \tag{13}$$

By the time we have checked all possible matrix products (always multiplying on the right onto existing words) of length 5, and using the identities and forbidden words as they appear, in this example, we find that we have exhausted the list of possible combinations, thus closing the search. We can accumulate this list of allowed words as vertices of a graph as depicted in Fig. 8, and then considering right multiplying by an A or B matrix gives a transition to another vertex by considering the list of identities. We know that we have completed the lists when all possible transitions have been accounted for. Note that this semigroup graph is not irreducible, but there are three irreducible subgraphs, each of which are dynamically identical.

Before we get to the main result of this section, let us make the following observation about the semigroup graphs.

Proposition 6.2. *The semigroup construction produces a graph which is a right-resolving presentations of the underlying sophic shifts.*

Proof. This follows essentially by construction. Consider a product of A and B matrices which make an allowed matrix word X. Then assuming $A \neq B$, then $X \cdot A \neq X \cdot B$. Therefore, every vertex labeled X has a distinct A and B edge. (We do not show edges which come from forbidden words $X \cdot A = \mathbf{0}$ or $X \cdot B = \mathbf{0}$.) □

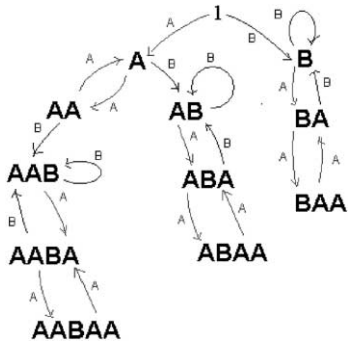

Fig. 8. Semigroup graph of non-zero matrix products and transition product identities from the odd shift. This graph is a right-resolving presentation of the graph shown in Fig. 7.

The odd shift was chosen for simplicity, because its lists of identities are short, and its transition matrices are only 3×3 and hence easy to exhaust by hand calculation. For our sequences of misplaced partitions, and corresponding sequences of sophic shifts, the corresponding semigroup matrices can be constructed in closed form with the aid of a computer algebra system. The above proposition implies that the semigroup graphs could be used in the place of the algorithm of the previous section in exactly calculating the $h_T(d)$ function. It is generally more computationally expensive this way.

The semigroup graph is most useful to determine the question if a subshift is of infinite type or to produce the complete set of minimal forbidden words. Motivated by the odd shift example, we now show how to detect a grammar of infinite type.

Theorem 6.1 (Minimal forbidden words). *Let d_1 and d_2 be letters from the set $\{a, b\}$ (more generally, they could be letters from a larger alphabet), and let D_1 and D_2 be the semigroup matrices representing these letters. Let w be a word in the alphabet $\{a, b\}$, and let X be the semigroup matrix which represents w. Then $d_1 w d_2$ is a minimal forbidden word if and only if the following three conditions hold*:

1. $D_1 \cdot X \neq \mathbf{0}$;
2. $X \cdot D_2 \neq \mathbf{0}$;
3. $D_1 \cdot X \cdot D_2 = \mathbf{0}$.

Proof. Suppose that (1)–(3) hold. $D_1 \cdot X \cdot D_2 = 0$ implies that the word $d_1 w d_2$ is forbidden. No proper subword of $d_1 w d_2$ can be forbidden, because any proper subword of $d_1 w d_2$ is either a subword of $d_1 w$ or a subword of $w d_2$, and neither of these are forbidden. Thus $d_1 w d_2$ is a minimal forbidden word. Now suppose that $d_1 w d_2$ is a minimal forbidden word. Because $d_1 w d_2$ is forbidden, $D_1 \cdot X \cdot D_2 = 0$. No proper subword of $d_1 w d_2$ is forbidden, so neither $d_1 x$ nor $x d_2$ are forbidden, so neither $D_1 \cdot X$ nor $X \cdot D_2$ is equal to 0. □

Theorem 6.2 (Grammar of infinite type). *A subshift is of infinite type if and only if there exist letters d_1 and d_2 represented by semigroup matrices D_1 and D_2, as in Theorem* 6.1, *and a semigroup matrix X, such that the following four conditions hold*:

1. $D_1 \cdot X \neq \mathbf{0}$;
2. $X \cdot D_2 \neq \mathbf{0}$;

3. $D_1 \cdot X \cdot D_2 = \mathbf{0}$;
4. *There exist an infinite number of words w represented by the matrix X.*

Proof. Following Theorem 6.1, a minimal forbidden word is given by a product $D_1 \cdot X \cdot D_2$, satisfying (1)–(3), corresponding to a word $d_1 w d_2$. There are only a finite number of possibilities for each of D_1, X, and D_2, because there are only a finite number of matrices in the semigroup. The only way to have an infinite list of forbidden words is that there to be an infinite number of words w associated with one of the matrices X. □

Table 1
Table of grammar changes of the symbols sequence generated by the tent map due to changing the misplacement parameter $d = (k/2^n)$. Shown are the minimal forbidden words, characteristic polynomial, Perron number, and topological entropy of the symbols sequences

k	n	d	Minimal forbidden words	Polynomial	Perron number	Entropy
−16	1	$-\frac{16}{32}$	A	$z-1$	1	0
−15	5	$-\frac{15}{32}$	ABA, ABBA, ABBBA, ABBBBA	$(z^3-z^2-1)(z^3-z^2+1)$	1.46557123	0.38224509
−14	4	$-\frac{14}{32}$	ABA, ABBA, ABBBA	$(z^5-2z^4+z^3-1)$	1.52894635	0.42457884
−13	5	$-\frac{13}{32}$	ABA, ABBA, ABBBA	$(z^5-2z^4+z^3-1)$	1.52894635	0.42457884
−12	3	$-\frac{12}{32}$	ABA, ABBA	$(z^2-z+1)(z^2-z-1)$	1.61803399	0.48121183
−11	5	$-\frac{11}{32}$	ABA, ABBA, ABBBBA	$(z^6-2z^5+z^4-z^2+z-1)$	1.56175207	0.44580831
−10	4	$-\frac{10}{32}$	ABA, ABBA	$(z^2-z+1)(z^2-z-1)$	1.61803399	0.48121183
−9	5	$-\frac{9}{32}$	ABA, ABBA	$(z^2-z+1)(z^2-z-1)$	1.61803399	0.48121183
−8	2	$-\frac{8}{32}$	ABA	(z^3-2z^2+z-1)	1.75487767	0.56239915
−7	5	$-\frac{7}{32}$	ABA, ABBBAA, ABBBABBB	$(z^8-2z^7+z^6-z^5+z^4-z^3-z+1)$	1.69130569	0.52550083
−6	4	$-\frac{6}{32}$	ABA, ABBBA	$(z^5-2z^4+z^3-z^2+z-1)$	1.67364855	0.51500600
−5	5	$-\frac{5}{32}$	ABA, ABBBA	$(z^5-2z^4+z^3-z^2+z-1)$	1.67364855	0.51500600
−4	3	$-\frac{4}{32}$	ABA	(z^3-2z^2+z-1)	1.75487767	0.56239915
−3	5	$-\frac{3}{32}$	ABAA, ABABBA, ABABBBB, ABABBBABA	$(z^9-2z^8+z^6-z^5+z^4-z^2+z-1)$	1.78720696	0.58065404
−2	4	$-\frac{2}{32}$	ABAA	(z^4-2z^3+z-1)	1.86676039	0.62420452
−1	5	$-\frac{1}{32}$	ABAAA	(z^5-2z^4+z-1)	1.93318499	0.65916889
0	1	0	None	$(z-2)$	2	0.69314718
1	5	$\frac{1}{32}$	BBAAAA, BBAAABB, BBAAABAB, BBAAABAAB	$(z^9-2z^8+z^4-1)$	1.93357727	0.65937180
2	4	$\frac{2}{32}$	BBAAA, BBAABB, BBAABAB	$(z^7-2z^6+z^3-1)$	1.87055662	0.62623604
3	5	$\frac{3}{32}$	BBAA, BBABB	$(z^5-2z^4+z^2-1)$	1.78459894	0.57919370
4	3	$\frac{4}{32}$	BBAA, BBABB	$(z^5-2z^4+z^2-1)$	1.78459894	0.57919370
5	5	$\frac{5}{32}$	BBAA, BBABB, BBABAA, BBABABB	$(z^7-2z^6+z^4-1)$	1.69378496	0.52696565
6	4	$\frac{6}{32}$	BB	(z^2-z-1)	1.61803399	0.48121183
7	5	$\frac{7}{32}$	BB	(z^2-z-1)	1.61803399	0.48121183
8	2	$\frac{8}{32}$	BB	(z^2-z-1)	1.61803399	0.48121183
9	5	$\frac{9}{32}$	BB	(z^2-z-1)	1.61803399	0.48121183
10	4	$\frac{10}{32}$	BB, BAB	(z^3-z^2-1)	1.46557123	0.38224509
11	5	$\frac{11}{32}$	BB, BAB	(z^3-z^2-1)	1.46557123	0.38224509
12	3	$\frac{12}{32}$	BB, BAB	(z^3-z^2-1)	1.46557123	0.38224509
13	5	$\frac{13}{32}$	BB, BAB, BAAB	(z^4-z^3-1)	1.38027757	0.32228462
14	4	$\frac{14}{32}$	BB, BAB, BAAB	(z^4-z^3-1)	1.38027757	0.32228462
15	5	$\frac{15}{32}$	BB, BAB, BAAB, BAAAB	$(z^2-z+1)(z^3-z-1)$	1.32471796	0.28119957
16	1	$\frac{16}{32}$	B	$z-1$	1	0

In the case of the odd shift, the semigroup matrix representing the word *aa* also represents an infinite number of other words, by the identity $A \cdot A \cdot A = A$ found in Eq. (11). Moreover, *BAA* and *AAB* are not forbidden, but *BAAB* is, and therefore the odd shift is not of finite type.

To analyze the grammar of a subshift, then, we first find all possible triples D_1, X, and D_2, satisfying conditions (1)–(3). For each such X, we can either write down the list of words w that are represented by X, or else we can say that the list is infinite. This is because words w represented by X correspond to paths in the semigroup graph which begin at 1 and end at X. If there is any X representing an infinite number of words w, then the grammar is infinite. Otherwise, it is finite, and we produce a complete list of the minimal forbidden words.

Now back to our tent map problem. We have written a computer program which carries out the semigroup construction for each of a sequence of misplaced partition sophic shifts $\Sigma_2^{\{a,b\}}(d)$ for a sequence of dyadic $d = q/2^n$ for $q = 1, 2, \ldots, 2^n$, and successfully for up to $n = 16$. For reasons of brevity, we have only tallied for $n \leq 5$ the complete list of forbidden words for each corresponding sophic shift in Table 1. In Appendix B, we give the complete details and the graphical presentation of the semigroup arising from the sophic shift due to a simple dyadic misplacement.

Remark 6.2. A grammar of infinite type first occurs for $n = 6$ with $d = \frac{7}{64}$, not shown in our table for reasons of brevity. The list grows quickly with n.

7. Explanation of non-monotonicity by masking functions

In Section 6, we used "masking" matrices A and B to determine if any walks through the re-labeled graph $\mathcal{G}$ permits a corresponding $a; b$ word, according to Theorem 6.1 (grammar characterization by matrices). In this section, we will mimic this construction directly within the tent map equation (1) by defining a map which masks those points which do not have a desired itinerary.

Let χ_A be the following characteristic function defined on the unit square, $x \in [0, 1]$, $p \in [0, 1]$

$$\chi_A(x, p) = \begin{cases} 1 & \text{if } x < p, \\ 0 & \text{else.} \end{cases} \tag{14}$$

Likewise define

$$\chi_B(x, p) = 1 - \chi_A(x, p). \tag{15}$$

Now define

$$A(x, p, i) = T^i(x)[\chi_A(x, p) \circ T^i(x)], \quad i \geq 0, \tag{16}$$

and likewise

$$B(x, p, i) = T^i(x)[\chi_B(x, p) \circ T^i(x)], \quad i \geq 0, \tag{17}$$

where we denote for consistency $T^0(x) \equiv x$ meaning the identity map. With these maps of the Cartesian product of the unit interval by the unit parameter interval, we can state the following masking proposition.

Proposition 7.1. *The set of* $(x, p) \in [0, 1] \times [0, 1]$ *such that the symbol "a" occurs in the ith-bit in the p-partition itinerary of x, according to Eqs.* (3) *and* (4), *coincides with* $A(x, p, i) > 0$. *Likewise* $B(x, p, i) > 0$ *coincides with all* (x, p) *with a "b" symbol in the ith-bit of its p-partition itinerary.*

Proof. The construction defined by notation, Eqs. (14)–(17), agrees with the definition of p-partition symbols, Eqs. (3) and (4). □

Corollary 7.1 (Grammar characterization by masking functions). *Consider an* $n+1$*-bit word* $w = d_0 d_1 \cdots d_n$, *where* $d_j = a$ *or* b. *Define for each symbol* d_j, *the like labeled function* $D(x, p, j) = A(x, p, j)$ *or* $B(x, p, j)$. *The set of* $(x, p) \in [0, 1] \times [0, 1]$ *such that* w *occurs in the* p*-partition itinerary of* x, *according to Eqs.* (3) *and* (4) *coincides with those* (x, p) *such that* $\prod_{i=0}^{n} D(x, p, i) > 0$.

Proof. This follows immediately Proposition 7.1. □

Remark 7.1. Since no matrices are need to describe existence of specific words in $\Sigma_2^{\{a,b\}}(p)$ in this way, the previous restriction of p to rational values is not necessary.

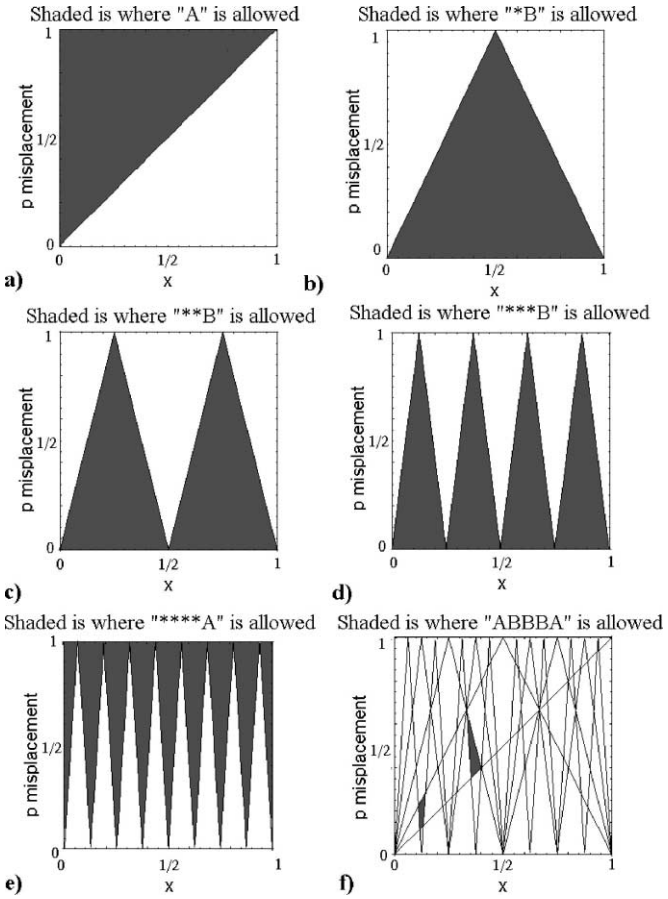

Fig. 9. Masking decides a words life through varying p: (a) dark shows $(x, p) \in [0, 1] \times [0, 1]$ such that its p-partition itinerary admits an a in the first bit; (b) dark shows (x, p) set with b in second bit; (c) and (b) dark shows (x, p) set with b in third bit; (d) dark shows (x, p) set with b in fourth bit; (e) dark shows (x, p) set with a in fifth bit; (f) an intersection of the dark regions (non-zero supports) gives the disconnected region shown which supports the word *abbba*.

On one hand, Corollary 7.1 allows for a succinct way to characterize the life of a word through varying p. On the other hand, to evaluate easily Eqs. (16) and (17), we must eventually resort to iterating the map for many initial conditions, which brings us back to Eqs. (3) and (4). Nonetheless, for small word lengths, it is possible to find boundaries of the non-zero support as the intersections of several lines.

A given word is a specific "stacking" of these "templates" which decides the p-range for a given word. We have built such a stacking crudely with paper and scissors from Fig. 9, for example. Consider the word *abbba* which we already demonstrated by relabeling graphs in Section 4, Example 4.3, exhibits a non-monotonicity. In Fig. 9, we display a series of masks for each of the letters in the given position, which has a non-zero support who's intersection is depicted in Fig. 9f. The main point of this example is that we again see the non-monotonicity realized as two distinct regions of *ABBBA* which exhibit an interval of p separation. In other words, a horizontal band fits between the red regions.

Inspection of Fig. 9 gives some geometric intuition of the dynamical cause of non-monotonicity. It is not uncommon for a composition of masks to create a disconnected word region in the (x, p) unit box. Consider, for example that the interiors of masks B, $*B$ and $**B$ are disconnected, but that does not cause a non-monotonicity by itself. The other important feature is that a horizontal strip, $\exists 0 < p_1 < p_2 < 1$ such that $\{(x, p), p_1 \leq p \leq p_2\}$, can be placed in between the two disconnected regions of the unmasked word *abbba*. The reason for this vertical space is due to a mix of shallow (early iterate) and steep (late iterate) masking.

8. Nonuniqueness of a; b labelings

In this section, we consider the extent to which a misplaced partition can result in non-unique a; b names for the points of the unit interval. It is well known that by not choosing a generating partition, two distinct points of the dynamical system will not necessarily have distinct symbolic names [4]. [3] Consider the tent map, Eq. (1), and the misplaced partition, Eq. (4), with $d = p - \frac{1}{2} \neq 0$. If $0 < x < d$, then $\frac{1}{2} + x$ lies on the same side of p as $\frac{1}{2} - x$, and since $f(\frac{1}{2} + x) = f(\frac{1}{2} - x)$, we see that $\varphi_i(\frac{1}{2} + x) = \varphi_i(\frac{1}{2} - x)$ for all $i \geq 0$, and thus the interval $(\frac{1}{2} - d, \frac{1}{2})$ is undistinguished by a; b words from the interval $(\frac{1}{2}, \frac{1}{2} + d)$.

Consider for a moment the case $p = \frac{1}{4}$. Let $C_{1/4}$ be the set of all initial conditions $x \in [0, 1]$ such that the orbit of x never visits the interval $[0, \frac{1}{4})$. The elements of $C_{1/4}$ are characterized by having 0; 1 sequences $\sigma(x)$ which contain no two consecutive occurrences of 0. Moreover, the elements of $C_{1/4}$ are exactly those whose a; b sequences are $b \cdot \bar{b}$. More generally, we can say exactly when two initial conditions $x, y \in [0, 1]$ have the same a; b sequence.

Proposition 8.1. *An "a" occurs in the sequence $\varphi(x)$ exactly when there are two consecutive occurrences of* 0 *in* $\sigma(x)$.

A run of k occurrences of a in $\varphi(x)$ corresponds to a run of $k+1$ occurrences of 0 in $\sigma(x)$. Therefore, $\varphi(x) = \varphi(y)$ if and only if $\sigma(x)$ and $\sigma(y)$ have matching runs of zeros of length >1. (When $p = 1/2^n$, then it can be similarly shown that $\varphi(x) = \varphi(y)$ if and only if $\sigma(x)$ and $\sigma(y)$ have matching runs of zeros of length $\geq n$.)

Example 8.1. The following words are $p = \frac{1}{4}$ indistinguishable (since exchanging 111 and 101 do not effect the a; b word), at least up to the finite number of bits shown

[3] A measure theoretic definition of *generating partition* can be found in [4]. Given a dynamical system $\mathbf{f} : M \to M$ on a measure space (M, F, μ), a finite partition $P = \{B_i\}_{i=0}^{k}$ is generating if the union of all images and preimages of P give the set of all μ-measurable sets F. In other words, the "natural" tree of partitions: $\bigvee_{i=-\infty}^{\infty} \mathbf{f}^i(P)$, always generates some sub-σ-algebra, but if it gives the full σ-algebra of all measurable sets F, then P is called *generating* [4].

$$\varphi(x) = \overbrace{0.000}^{a's}\overbrace{101011110}^{b's}\overbrace{0}^{a}\cdots, \tag{18}$$

$$\varphi(y) = \overbrace{0.000}^{a's}\overbrace{111110110}^{b's}\overbrace{0}^{a}\cdots. \tag{19}$$

In the above example, the first sequence may be transformed into the second by several replacements of 111 with 101, or vice versa. Such a replacement never changes the a; b sequence. Most initial conditions $x \in [0, 1]$ have an infinite number of distinct, non-overlapping occurrences of 111 and/or 101 in their 0; 1 expansions. Such an x is then $\frac{1}{4}$-undistinguishable from an uncountable number of other initial conditions. To see this, let z be an arbitrary infinite binary sequence, say on the letters s and t. Use z to modify x as follows. Number the occurrences of 111 and 101 in $\sigma(x)$ with the positive integers. Then, if $z_i = s$, switch occurrence number i, 111 to 101 or vice versa, and if $z_i = t$, do not switch. Each binary sequence z produces a distinct new initial condition x_z, with $\varphi(x) = \varphi(x_z)$. Since there are an uncountable number of binary sequences z, there are also an uncountable of conditions x_z which are $\frac{1}{4}$-undistinguishable from x. (Note that this construction does not necessarily produce all the conditions y which are undistinguishable from x.)

For an arbitrary value of p, it is much more complicated to attempt to describe all cases of $\varphi(x) = \varphi(y)$ for $x, y \in [0, 1]$. However, it turns out that when p is dyadic, we can generalize the idea of replacing one string of finite length with another without changing the a; b sequence, as we shall see in the proof of the next theorem. We say that an initial condition x is *uncountably p-undistinguished* if there exist an uncountable number of distinct initial conditions y such that $\varphi(x) = \varphi(y)$ when the partition is set at p. Note that if the set of all uncountably p-undistinguished conditions is non-empty, then it must be uncountable.

Theorem 8.1. *If $p = q/2^n \neq \frac{1}{2}$, then the set of uncountably p-indistinguished initial conditions is dense in* [0,1].

Proof. Given p, the idea is to construct a pair of finite-length words w_1 and w_2 (analogous to the 111 and 101 exchange valid when $p = \frac{1}{4}$ as in Example 8.1), such that replacing one with the other in an expansion $\sigma(x)$ does not change $\varphi(x)$. Because $p = q/2^n$, whether $x > p$ or $x < p$ depends only on the first n0; 1 bits $\sigma_0(x), \sigma_1(x), \ldots, \sigma_{n-1}(x)$. First, suppose that $p < \frac{1}{2}$, and let $w_1 = 1^n 110^{n-2}$, $w_2 = 1^n 010^{n-2}$. Now suppose that $x_1, x_2 \in [0, 1]$ differ only by an occurrence of w_1 in $\sigma(x_1)$ and w_2 and $\sigma(x_2)$. Because the first difference between w_1 and w_2 occurs after n-bits, we need only consider the situation where the w_i occur at the beginning of the x_i. So, suppose that $\sigma(x_1) = w_1 y_1$ and $\sigma(x_2) = w_2 y_2$, where y_1, y_2 are infinite 0; 1 sequences. We consider $\varphi_i(x_1)$ and $\varphi_i(x_2)$ in three possible cases:

- *Case* 1: $0 \leq i < n$. Then $\sigma_i(x_1) = \sigma_i(x_2) = 1$, so $f^i(x_1) > \frac{1}{2}$ and $f^i(x_2) > \frac{1}{2}$, and therefore since $p < \frac{1}{2}$, $\varphi_i(x_1) = \varphi_2(x_2) = b$.
- *Case* 2: $i > n$. Then $f^i(x_1) = f^i(x_2)$, so $\varphi_i(x_1) = \varphi_i(x_2)$.
- *Case* 3: $i = n$. Then $\sigma(f^i(x_1)) = 1.10^{n-2}y_1$ and $\sigma(f^i(x_2)) = 0.10^{n-2}y_2$. This means that $f^i(x_1)$ lies between 1/2 and $1/2 + 1/2^n$ and that $f^i(x_2)$ lies between $1/2 - 1/2^n$ and 1/2. Since $p \neq \frac{1}{2}$, this implies that $f^i(x_1)$ and $f^i(x_2)$ lie on the same side of p as one another, so $\varphi_i(x_1) = \varphi_i(x_2)$.

When $p > \frac{1}{2}$, then choose $w_1 = 0^n 110^{n-2}$ and $w_2 = 0^n 010^{n-2}$. The argument is essentially the same in this case, except that $f^i(x_1) < \frac{1}{2} < p$ and $f^i(x_2) < \frac{1}{2} < p$ for $1 \leq i \leq n$.

Given any $x \in [0, 1]$, we may choose $y \in [0, 1]$ arbitrarily close to x, such that y has infinitely many distinct, non-overlapping occurrences of w_1 in its 0; 1 expansion. By the same argument as in the case $p = \frac{1}{4}$, there are an uncountable number of distinct initial conditions which can be made from x by replacing w_1 with w_2 in some of the positions. □

9. Motivation and application

A generating partition is unfortunately difficult to find and justify in the most practical settings [10,12,13,26,27] in which the physical scientist has before them only a data stream measured from some oscillating experiment. Nonetheless, a popular way of obtaining symbolic dynamics is to use the so-called "threshold crossings" method [13]. In this section, we question the validity of such a method by relating our results to a more general case.

The central question is this: can we replace characterization of the dynamical process directly from the experimental measurements with the simpler problem of characterization of the bit stream of an arbitrary partition, without any essential loss of information about the original dynamical system. We have already rigorously shown in the preceding that at least in the case of a one hump map which generates the data stream, misplacing the partition has severe, non-intuitive and complex consequences. In fact, a recent application in chaotic cryptography makes use of this fact, in which the partition is *deliberately* misplaced as a cryptic key [28].

Consider a significantly more difficult example in which there is a point transformation in two dimensions. We discuss the Hénon map [29] because we consider it to be typical of what is likely to arise in physically relevant data sets, in that it is non-uniformly hyperbolic and multivariate.

Consider the analogy to threshold crossings in which we can sample a finite length data stream $\{(x_i, y_i)\}_{i=0}^{N}$ and we wish to convert these numbers to binary bits, by threshold crossings to some partition curve at $y = c$. To each measurement $y_i, n \leq i \leq N - n$, associate a $2n$-bit word $w_{2n} = \sigma_{-n} \cdots \sigma_{-1} \cdot \sigma_0 \cdots \sigma_{n-1}$

$$\sigma_j(x) = \begin{cases} 0 & \text{if } \ y_{i+j} < c \ \text{ for } \ -n \leq j \leq n-1, \\ 1 & \text{else for } \ -n \leq j \leq n-1, \end{cases} \tag{20}$$

allowing for an arbitrary partition, we consider a family of curves $y = c$ which horizontally stripe the attractor, noting that *none of them are generating*. Now, we produce in Fig. 11 an analogous topological entropy versus c function, $h_T(c)$ as in Fig. 2 which was also calculated numerically using a densely wandering orbit.

What makes the Hénon map a particularly good benchmark example is that it has what has become a widely accepted conjectured generating partition, which is the line segments connecting "primary" homoclinic tangencies [7]. See Fig. 10 depicting this generating partition in bold, and a few iterates and pre-iterates which demark 4-bit neighborhoods covering the attractor. Furthermore, the well studied symbolic dynamics of this map, have been argued to be partially ordered relative to a partially ordered maximal "pruning front" [5,7,30] in analogy to the kneading theory of one-dimensional maps. Therefore, we can in principle order symbolic neighborhoods naturally relative to this "true" partition, and then rename them in a systematic fashion to mimic a family of threshold crossings.

We believe, but cannot prove, that the mechanisms behind the appearance of Figs. 2 and 6 for the misplaced partitions of the tent map are analogous to those behind the obviously similar appearance of Fig. 11. Furthermore, we believe that this mechanism is ubiquitous and in the following sense, dimension independent. In short, the dynamical system is either Markov, or may be approximated by a Markov system, which when presented by a directed graph, a misplaced partition may be described as a relabeling of vertices with consequences to the resulting sophic shift described herein. We also believe that non-uniqueness problems are ubiquitous. Numerically reproducing a figure similar to Fig. 11, directly in symbol dynamics, requires defining the n-bit neighborhoods relative to the generating partition of the Hénon map, sorting them on their y-coordinate location, and then relabeling them successively based on this order. The difficulty is to decide how to perform this y-sort when n is not so large that a good ordering is obvious. The difficulty is especially apparent in Fig. 10 in which when comparing the 4-bit neighborhoods, such as 1100 and 0100, it is not obvious which to rename first upon increasing y.

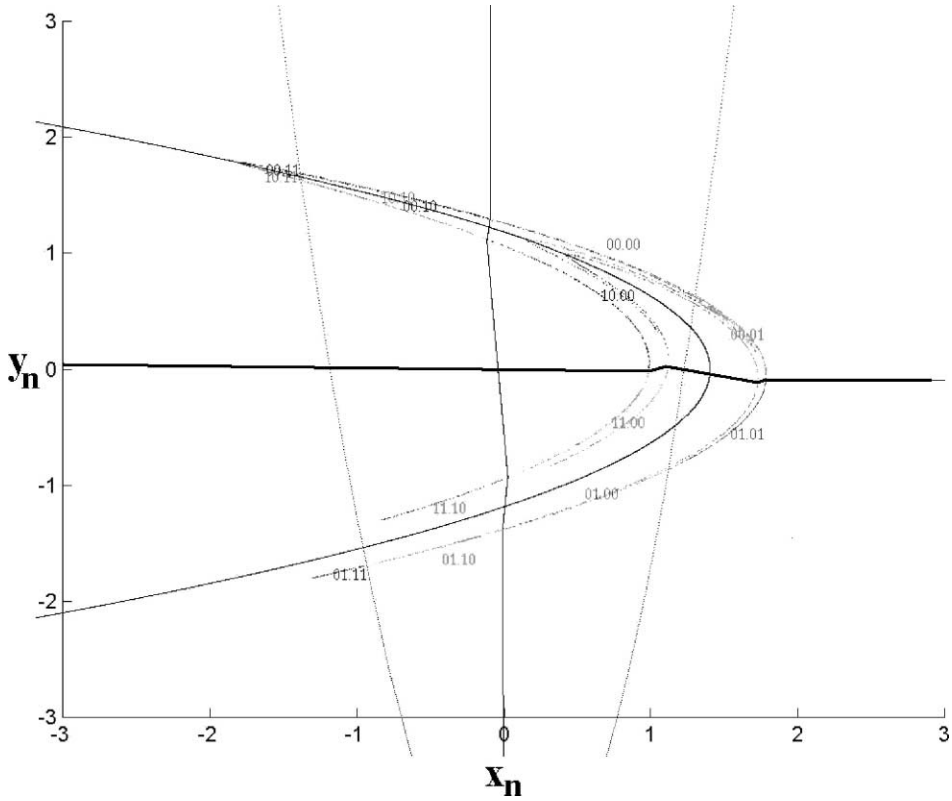

Fig. 10. The Hénon map, $x_{n+1} = a - x_n^2 + by_n$, $y_{n+1} = x_n$, where $a = 1.4$, $b = 0.3$. The generating partition connecting homoclinic tangencies is boldly depicted. Also shown are enough iterates and pre-iterates of this partitioning curve to delineate the 4-bit neighborhoods covering the attractor.

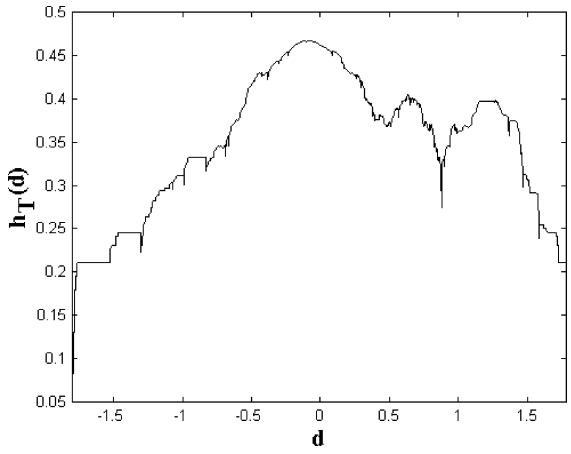

Fig. 11. Topological entropy of the Hénon map due to a family misplaced partitions given by horizontal lines $y = c$ for $-2 \leq c \leq 2$. Compare these horizontal line partitions to the "true" conjectured partition shown in Fig. 10.

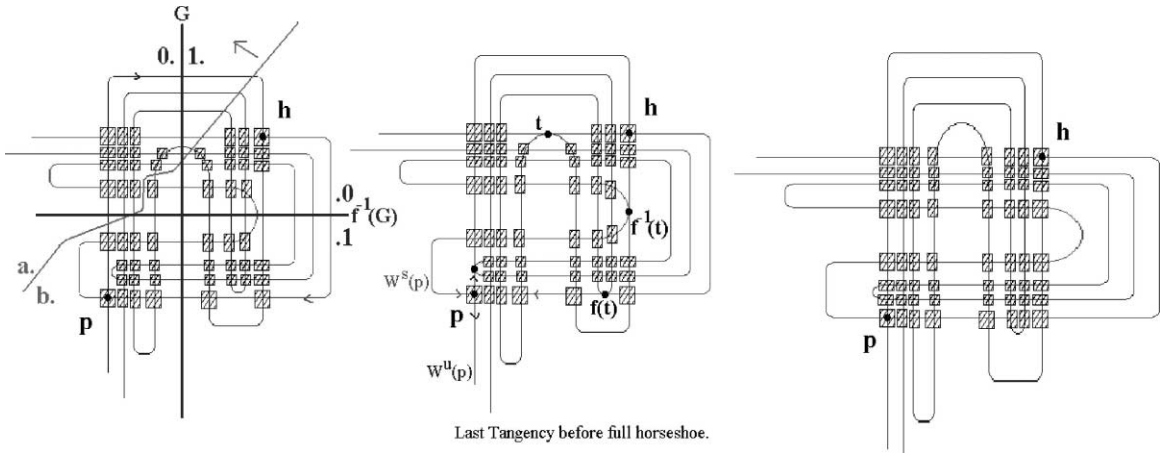

Fig. 12. Unfolding of the last tangency homoclinic bifurcation before a full horseshoe. We contrast between a generating partition (vertical curve labeled G) and an arbitrary partition (cutting diagonally across the figure). This arbitrary partition may well be a straight line threshold crossing under an appropriate change of coordinates, as will the stable/unstable manifolds and generating partitions become curves. Labeled are: the fixed point (**p**), its stable and unstable manifolds ($W^{\mathrm{s}}(\mathbf{p})$ and $W^{\mathrm{u}}(\mathbf{p})$), the primary transversal homoclinic point (**h**), points of tangency (**t** and iterates), and the generating partition (**G**).

In Fig. 12, we have attempted to clarify the points of the previous paragraph, by showing a specific example topology of a generating partition in a homoclinic tangle, and an arbitrary partition. We show the unfolding of the last tangency homoclinic bifurcation before a full horseshoe. At tangency (middle) the vertical line labeled "G" through the single "primary" homoclinic tangencies is generating [7], and we shown this partition in the left image, slightly pulled back from tangency. Notice that the subshift in the left shown tangle includes only fifty-six 4-bit words, while the fullshift (right) has 64, since pairs of words collide and are destroyed at tangency. These cartoons of unfolding a tangency bifurcation are not typical of a homoclinic tangle arising from a map such as Hénon, since the stable and unstable manifolds are normally curves, not straight lines. We have also shown (left) a possible "arbitrary" partition cutting diagonally between the 4-bit labeled neighborhoods, de marking (a; b) misplaced words, and a direction in which a family of such curves might move. A change of coordinates which would carry this arbitrary curve to a straight line (perhaps a threshold crossing) would also carry the stable and unstable manifolds, and the generating partition into curves. For this reason, we say that we do not expect a threshold crossing to be generating. It is easy to see in Fig. 12 that the arbitrary partition shown has a grammar which can be found by considering relabeling a directed graph on 56 vertices, as described here for the tent map.

We hope that we have shed some light on the consequences of possible misplacement of partitioning curves relative to the of the well regarded conjectures for generating partition of the Hénon, standard, and billiards maps [7–9,36,37]. We consider this to be an important issue, since choosing an arbitrary partitioning curve has already become a common practice in the physical literature. It should be pointed out that Mischaikow et al. [31] have shown that it is possible to rigorously approximate symbol dynamics in the setting of experimental data, at least for a subset of the phase space. Finally, one of our original motivations was in the field of communication with chaos by controlling itinerary sequences [32,39–42], perhaps in an electronic or optical device whose dynamics do not reduce to a simple interval map; in fact, the dynamical system might be available only as data from experiment through time-series embedding [33]. A primary obstacle to realizing this application is then to develop symbol dynamics for the device.

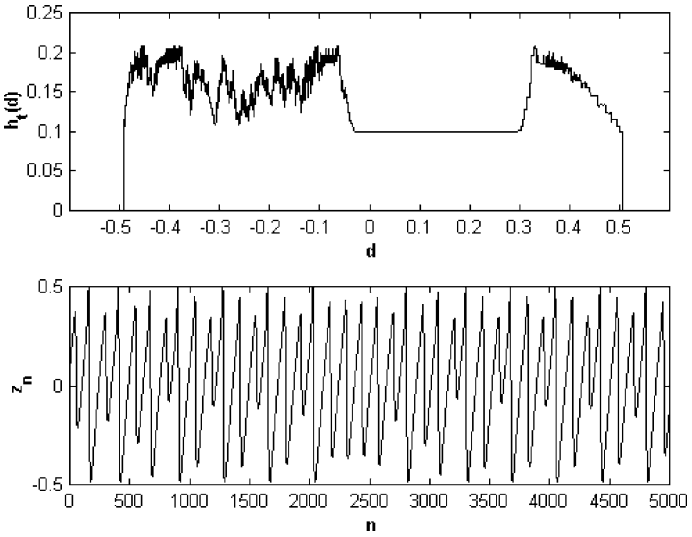

Fig. 13. (a) Topological entropy versus partition placement, $h_t(d)$ for experimentally collected chemical reaction (BZ) data. (b) Time-series of the data.

We conclude this section by showing an experimentally collected time-series of data measured from a chaotically oscillating Belousov–Zhabotinskii reaction [34], see Fig. 13. Time-delay techniques indicate a five-dimensional embedding. In any case, it is by no means obvious what form a generating partition might take in this high dimensional space, nor is it likely to be a simple threshold crossing in the single time-series shown. A particularly interesting feature in this topological entropy misplacement graph is the prominent flat region for $0 \leq d \leq 0.3$. This feature is partially explained by direct inspection of the time-series, and noting that there are no critical points in this range. What we find to be particularly interesting by this feature is that while it might seem natural to place a threshold crossing in this "middle" range, such a position corresponds to a greatly reduced dynamical representation.

We emphasize that it is also not fair to choose the partition to be the position of maximal threshold crossing entropy. We do not in fact know how many symbols label a generating partition. As a simple indication of the possible seriousness implied by a bad arbitrary partition, note that if we have a dynamical system which is conjugate to a full 5-bit shift, say $x_{n+1} = 5x_n \bmod 1$, then the topological entropy is $\ln 5$. Suppose we partition into two parts. At best, the resulting shift dynamics can have a maximal topological entropy of $\ln 2$. Even if the generating partition does have just two elements, such as with the Hénon map, the generating partition does not likely to correspond any threshold.

10. Technical summary

Our principal result is that the entropy can be a non-monotone and devil's staircase-like function of the misplacement parameter. As such, the consequence of a misplaced partition can be severe, including significantly reduced topological entropies and a high degree of non-uniqueness.

We have focused our work on the tent map for which our results could be stated as mathematically rigorous. Our formalism to study a dyadic rationally misplaced partition is to consider the corresponding directed graph presentation, the so-called sophic shift, and then to re-label the vertices of this graph accordingly. We showed the fundamental mechanism behind the surprising non-monotonicity feature of the misplacement entropy function is

the loss of a label on a particular path, whence the label is lost entirely for awhile, but later becomes the label for some other path upon further misplacement (see Example 4.3). Using this framework, we discussed that the right-resolving presentation of the relabeled graph is necessary so that we might calculated entropy by the ln of the spectral radius of the transition matrix. Therefore, we presented a sufficient and finitely terminating algorithm, equivalent to the subset construction, to find such a presentation (see Section 5). We also presented an algorithm which gives an alternative presentation of the sophic shift, which we called the semigroup graph (see Section 6). The semigroup construction not only allows us to present the shift as a graph, but also to list all minimal forbidden words of the grammar of the misplaced partition, if the shift is of finite type. If the shift is not of finite type, we gave necessary and sufficient conditions which will arise in the process of running the semigroup construction. We generalized the ideas of the semigroup construction to a continuous analogue, which we called masking functions (see Section 7). This was a simple idea in that it could literally be built with construction paper, and scissors, and yet gives deep insight as to the fundamental mechanism behind the non-monotonicity of the misplacement entropy function. We investigated topological properties of the separation of points under a misplaced partition, which causes a high degree of non-uniqueness under the mislabeling (see Sections 8 and 9). In Section 8, we proved for $p = \frac{1}{4}$ that not only is there non-uniqueness, but there exist infinitely many points with undistinguishable pairs, and furthermore, there exists points which have infinitely many undistinguishable pairs, and finally, the indistinguishability is a dense property in the unit interval for any $p < \frac{1}{2}$. This followed a simple observation that if the (not misplaced) symbolic itinerary of a point has a run of zero's, then between the runs of zero's, the alternative symbolic itinerary corresponds to a point whose misplaced $(a; b)$ word is identical. In Section 9, we showed that the results of Section 8 are general for any $p < \frac{1}{2}$ by a so-called enzyme construction. In Section 10, we discussed our larger motivation to planar maps, and to threshold crossing symbolic dynamics arising from a physical experiment. We presented numerical evidence using the Hénon map and also experimentally collected chemical reaction data that our results are likely more generally true, albeit not proven here. Our argument to this point is that most of our analysis for the tent map took place in symbol space, and hence the generality, but deciding when each relative symbolic bin is relabeled requires knowledge of the underlying order of neighborhoods to the (unknown) generating partition. While this order is unknown it does presumably exist. It is for this reason that we consider our tent map to be a good study for the general problem.

11. Conclusions

In this paper, we have made a general statement that a severe under-representation of a dynamical system may be made by using an arbitrary threshold crossing. We have done so by choosing the tent map as an example in which we were able to make all of our statements in a mathematically rigorous fashion. Our belief is that this example displays the typical situation, which is founded in the techniques of our analysis and proofs which essentially took place all in symbol space. We relied heavily on the well-known symbolic order of 1D maps, by using kneading theory. Essentially, once we know the order in which symbolic bins are renamed, we have a problem of "repainting" a graph. In principle, such should be equally applicable to higher dimensional dynamical systems. However, without knowledge of the order (pruning) in which symbolic bins are renamed, any rigorous analysis follows an only numerical calculation of the partition. Our work is meant to be a prototypical description of what can go wrong when choosing an arbitrary partition, in the situation that the generating partition is unknown. Without knowing the generating partition, an arbitrary partition tends to be grossly misplaced leading to a gross misrepresentation of the dynamical system. Hence, we offer the advice that threshold crossing result must be interpreted with extreme caution.

On the other hand, careful inspection of our topological entropy Figs. 2, 6, 11 and 12 apparently indicate that topological entropy versus partition displacement is a continuous function. We offer this as a conjecture for the tent map, which we are unable to prove at this time. For physical reasons, continuity is a highly desirable property. A conjecture for general dynamical system is that that a continuous family of partitioning curves leads to a corresponding continuous topological entropy function. A physical experiment such that even the slightest misplacement of naming states or partitioning leads to observations which are a gross misrepresentation of the full dynamical system is an undesirable property, to say the least, since there is always some measurement or specification error. Attempting to prove continuity for our tent map benchmark is an important subject of our ongoing research.

The issue of continuity of the topological entropy function with respect to partition placement is closely related to understanding the role of noise in the observed sample-path symbolic dynamics. Here, we have studied the role of an exactly misplaced partition. It has been shown that stochastic operator techniques can be used to study of the blurring effects of noise [15,16,38]. For example, Crutchfield and Packard have shown that fine structures of invariant measure blur at the noise threshold. The connection between stochastic and chaotic descriptions can be based on the concept of a fine Markov covering of the chaotic attractor as in Gallavotti et al. [35,43,44]. This serves as motivation to extend the combinatorial techniques we have developed here to quantitatively assess the accuracy of conditional probabilities based on Markov chain descriptions of chaotic attractors. Thus for these scientifically interesting problems regarding noise and measured understanding of a dynamical system's underlying complexity, we are motivated to pursue the continuity question and also the connections between stochastic and chaotic descriptions of chaotic dynamics in our future work.

Acknowledgements

EMB was supported by NSF under Grant Nos. DMS-9704639 and DMS-0071314. TBS was supported by NARC. YCL was supported by AFOSR under Grant No. F49620-98-1-0400 and by NSF under Grant No. PHY-9722156. KŻ is thankful to USNA for hospitality. The authors are thankful to Eric Kostelich, who provided the BZ data [34]. TBS and EMB would like to thank Mark Kidwell for helpful discussions. We would also like to thank the referees for carefully reading and helpful suggestions.

Appendix A

We finish Example 4.3, verify by checking cases that when $n = 4$, and $d = -\frac{3}{16}$, that there exists no paths labeled *abbba*, through the graph in Fig. 3.

To begin a word with the letter a, when $d = -\frac{3}{16}$, the path must begin at one of the following five vertices: $0000 \prec 0001 \prec 0011 \prec 0010 \prec 0110$. We consider all trees of paths from each of these, which either follow as a needed letter, or terminate prematurely.

- *Case* 1:

$$\overbrace{0000}^{a} \rightarrow \begin{array}{c} \overbrace{0000}^{a} \\ \text{-or-} \\ \overbrace{0001}^{a} \end{array} . \tag{A.1}$$

Thus, all such paths begin $aa\ldots$.

- *Case* 2:

$$\overbrace{0001}^{a} \rightarrow \begin{array}{c} \overbrace{0010}^{a} \\ \text{-or-} \\ \overbrace{0011}^{a} \end{array}. \tag{A.2}$$

Again, all such paths begin $aa\ldots$.

- *Case* 3:

$$\overbrace{0011}^{a} \overset{\text{considering } b \text{ branch}}{\longrightarrow} \overbrace{0111}^{b} \longrightarrow \begin{array}{ll} & \overbrace{1100}^{b} \\ \overbrace{1110}^{b} \longrightarrow & \text{-or-} \\ & \overbrace{1101}^{b} \\ \text{-or-} & \not\rightarrow a \\ & \overbrace{1110}^{b} \\ \overbrace{1111}^{b} \longrightarrow & \text{-or-} \\ & \overbrace{1111}^{b} \end{array} \tag{A.3}$$

For now on, since we agree to only consider paths which lead to a letter needed to complete the word *abbba*, we can suppress the ackward notation "$\overset{\text{considering } b \text{ branch}}{\longrightarrow}$". In the same vein, "$\not\rightarrow a$" means that the rest of the (eight of them) following paths result in an a *b*.

- *Case* 4:

$$\begin{array}{ll} & \overbrace{1010}^{b} \longrightarrow \begin{array}{ll} & \overbrace{0101}^{b} \not\rightarrow a \\ \text{-or-} & \\ & \overbrace{0100}^{b} \not\rightarrow a \end{array} \\ \overbrace{0101}^{b} \longrightarrow \text{-or-} & \\ & \overbrace{1011}^{b} \longrightarrow \begin{array}{ll} & \overbrace{0111}^{b} \not\rightarrow a \\ \text{-or-} & \\ & \overbrace{0110}^{a} \end{array} \\ \overbrace{0010}^{a} \longrightarrow \text{-or-} & \\ & \overbrace{1001}^{b} \longrightarrow \begin{array}{ll} & \overbrace{0011}^{a} \\ \text{-or-} & \\ & \overbrace{0010}^{a} \end{array} \\ \overbrace{0100}^{b} \longrightarrow \text{-or-} & \\ & \overbrace{1000}^{b} \longrightarrow \begin{array}{ll} & \overbrace{0001}^{a} \\ \text{-or-} & \\ & \overbrace{0000}^{a} \end{array} \end{array} \tag{A.4}$$

From which we conclude that there must be either two, or four *b*'s following an *a*: $a\overbrace{bb}^{2}a\cdots$, or, $a\overbrace{bbbb}^{4}a\cdots$.

- *Case* 5:

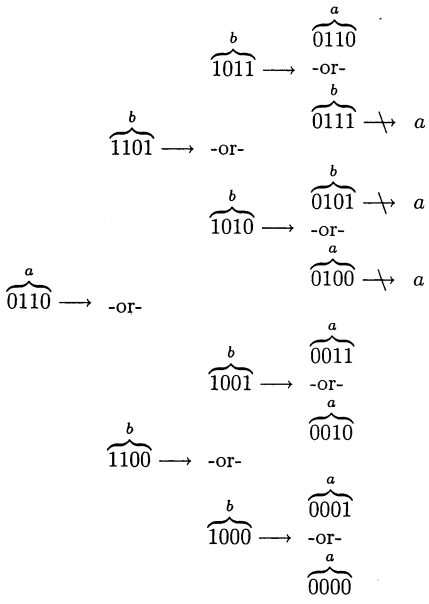

(A.5)

Again, we conclude two, or four b's follow an a: $a\overbrace{bb}^{2}a\cdots$, or, $a\overbrace{abbbb}^{2}a\cdots$.

We see that the shift $\Sigma_2^{\{a,b\}}(d)$ is strongly influenced by the underlying fullshift $\Sigma_2^{\{0,1\}}$.

Appendix B. Semigroup construction of a misplaced partition

In Section 6, we demonstrated the characterization of grammar by using the odd shift example, Fig. 7, which we chose to highlight because it demonstrated all interesting features, including that it generates a subshift of infinite type. In this section, we now show the details of the semigroup graph constructed for one of the simplest partition misplacements, which can come from our tent map subject to a misplaced partition, Eqs. (2) and (3). Let $d = -\frac{1}{4}$, which allows for a relabeling of the 4 vertex 2-bit graph, as depicted in Fig. 4. This directed graph has transition matrix

$$C = \begin{pmatrix} 1 & 1 & 0 & 0 \\ 0 & 0 & 1 & 1 \\ 0 & 0 & 1 & 1 \\ 1 & 1 & 0 & 0 \end{pmatrix}. \tag{B.1}$$

Again, considering each only those transitions carrying the label a or b gives

$$A = \begin{pmatrix} 1 & 0 & 0 & 0 \\ 0 & 0 & 0 & 0 \\ 0 & 0 & 0 & 0 \\ 1 & 0 & 0 & 0 \end{pmatrix}, \quad \text{and likewise} \quad B = \begin{pmatrix} 0 & 1 & 0 & 0 \\ 0 & 0 & 1 & 1 \\ 0 & 0 & 1 & 1 \\ 0 & 1 & 0 & 0 \end{pmatrix}. \tag{B.2}$$

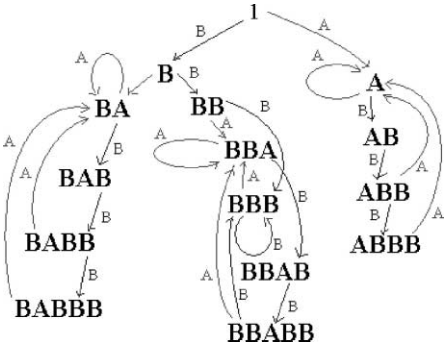

Fig. 14. Semigroup graph of non-zero matrix products and transition product identities from the misplaced partition of the tent map, $d = -\frac{1}{4}$, see Fig. 4 and Eq. (B.5).

All possible words starting with a and b follows by matrix multiplication and Proposition 6.1. Right multiplying by all possible (matrix) words of length 1, then 2, etc., gives the following set of identities, forbidden words, and new words, before the list terminates as a closed and consistent set of rules:

$$\text{Identities :} \quad A \cdot A = A, \quad A \cdot B \cdot B \cdot A = A, \quad B \cdot B \cdot B \cdot A = B \cdot B \cdot A, \quad B \cdot B \cdot B \cdot B = B \cdot B \cdot B, \tag{B.3}$$

$$\text{Forbidden :} \quad A \cdot B \cdot A = \mathbf{0}. \tag{B.4}$$

The exhaustive search for new words of ever longer length, and using the identities of longer length as they appear gives a list of allowed words:

$$\begin{aligned}\text{Allowed matrix words :} \quad & A\,, \quad B, \quad A \cdot B, \quad B \cdot A, \quad B \cdot B, \quad B \cdot A \cdot B, \quad B \cdot B \cdot A, \quad A \cdot B \cdot B, \\ & B \cdot B \cdot B, \quad A \cdot B \cdot B \cdot B, \quad B \cdot A \cdot B \cdot B, \quad B \cdot B \cdot A \cdot B.\end{aligned} \tag{B.5}$$

We have made no attempt to optimize this list, but rather for clarity, we have presented it in the order in which our hand calculations have presented it (Fig. 14).

References

[1] S. Smale, Differentiable dynamical systems, Bull. AMS 73 (1967) 747.
[2] R. Bowen, Equilibrium States and the Ergodic Theory of Anosov Diffeomorphisms, Springer, Berlin, 1975.
[3] P. Góra, A. Boyarsky, Laws of Chaos, Invariant Measures and Dynamical Systems in One Dimension, Birkhäuser, Boston, 1997.
[4] D.J. Rudolph, Fundamentals of Measurable Dynamics, Ergodic Theory on Lebesgue Spaces, Clarendon Press, Oxford, 1990.
[5] P. Cvitanovic, Periodic orbits as the skeleton of classical and quantum chaos, Physica D 51 (1991) 138.
[6] R. Mane, Ergodic Theory and Differentiable Dynamics, Springer, New York, 1987.
[7] P. Cvitanovic, G. Gunaratne, I. Procaccia, Phys. Rev. A 38 (1988) 1503.
[8] F. Christiansen, A. Politi, Guidelines for the construction of a generating partition in the standard map, Physica D 109 (1997) 32.
[9] K. Hansen, Symbolic dynamics: O. Finite dispersive billiards, Nonlinearity 6 (1993) 753.
[10] J. Kurths, A. Voss, P. Saparin, A. Witt, H. Kleiner, N. Wessel, Quantitative analysis of heart rate variability, Chaos 5 (1995) 88.
[11] C.S. Daw, M.B. Kennel, C.E.A. Finney, F.T. Connolly, Observing and modeling nonlinear dynamics in an internal combustion engine, Phys. Rev. E 57 (1998) 2811.
[12] R. Engbert, C. Scheffczyk, R. Krampe, J. Kurths, R. Kliegl, Symbolic dynamics of bimanual production of polyrhythms, in: H. Kantz, J. Kurths, G. Mayer-Kress (Eds.), Nonlinear Time Series Analysis of Physiological Data, Springer, Heidelberg, 1998, pp. 271–282.
[13] M. Lehrman, A.B. Rechester, Symbolic analysis of chaotic signals and turbulent fluctuations, Phys. Rev. Lett. 78 (1997) 1.

[14] E. Bollt, T. Stanford, Y.-C. Lai, K. Życzkowski, Validity of threshold-crossing analysis of symbolic dynamics from chaotic time series, Phys. Rev. Lett. 85 (2000) 3524.
[15] J.P. Crutchfield, N.H. Packard, Int. J. Theoret. Phys. 21 (1982) 433.
[16] A. Ostruszka, P. Pakoński, W. Słomczyński, K. Życzkowski, Dynamical entropy for systems with stochastic perturbations, Phys. Rev. E 62 (2000) 2018.
[17] C.M. Glenn, S. Hayes, Targeting regions of chaotic attractors using small perturbation control of symbolic dynamics, ARL-TR-903, May 1996.
[18] Hao Bai-Lin, Elementary Symbolic Dynamics, World Scientific, Singapore, 1989.
[19] B.P. Kitchens, Symbolic Dynamics, One-sided, Two-sided and Countable State Markov Shifts, Springer, New York, 1998.
[20] R.L. Devaney, An Introduction to Chaotic Dynamical Systems, 2nd Edition, Addison-Wesley, Reading, MA, 1989.
[21] C. Robinson, Dynamical Systems: Stability, Symbolic Dynamics, and Chaos, CRC Press, Ann Arbor, MI, 1995.
[22] E. Bollt, Y.-C. Lai, Dynamics of coding in communicating with chaos, Phys. Rev. E 58 (1998) 1724.
[23] K. Życzkowski, E. Bollt, Physica D 132 (1999) 393.
[24] J. Milnor, W. Thurston, On Iterated Maps of the Intervals I and II, Princeton University Press, Princeton, NJ, 1977.
[25] D. Lind, B. Marcus, An Introduction to Symbolic Dynamics and Coding, Cambridge University Press, New York, 1995.
[26] U. Schwarz, J. Kurths, A. Witt, A.O. Benz, Analysis of solar spike events by means of symbolic dynamics methods, Space Sci. Rev. 68 (1994) 245.
[27] M.B. Kennel, A.I. Mees, Testing for general dynamical stationarity with a symbolic data compression technique, Phys. Rev. E 61 (2000) 2563.
[28] E. Alvarez, A. Fernandez, P. Garcia, J. Jimenez, A. Marcano, New approach to chaotic encryption, Phys. Lett. A 263 (1999) 373.
[29] M. Hénon, Commun. Math. Phys. 50 (1976) 69.
[30] A. de Carvalho, Pruning fronts and the formation of horseshoes, Ergodic Theory Dyn. Syst. 19 (1999) 851.
[31] K. Mischaikow, M. Mrozek, J. Reiss, A. Szymczak, Construction of symbolic dynamics from experimental time series, Phys. Rev. Lett. 82 (1999) 1144.
[32] S. Hayes, C. Grebogi, E. Ott, Phys. Rev. Lett. 70 (1993) 3031.
[33] F. Takens, in: D. Rand, L.-S. Young (Eds.), Dynamical Systems and Turbulence, Lecture Notes in Mathematics, Vol. 898, Springer, Berlin, 1980, p. 366.
[34] R.H. Simoyi, A. Wolf, H.L. Swinney, Phys. Rev. Lett. 49 (1982) 245.
[35] G. Gallavotti, E. Cohen, Dynamical ensembles in stationary states, J. Statist. Phys. 80 (5–6) (1995) 931.
[36] F. Christiansen, A. Politi, Symbolic encoding in symplectic maps, Nonlinearity 9 (1996) 1623.
[37] K. Hansen, Pruning of orbits in four-disk and hyperbola billiards, Chaos 2 (1992) 71.
[38] J.P. Crutchfield, N.H. Packard, Symbolic dynamics of noisy chaos, Physica D 7 (1983) 201.
[39] E. Bollt, Y.-C. Lai, C. Grebogi, Coding, channel capacity, and noise resistance in communicating with chaos, Phys. Rev. Lett. 79 (1997) 3787.
[40] S. Hayes, C. Grebogi, E. Ott, A. Mark, Phys. Rev. Lett. 73 (1994) 1781.
[41] E. Rosa, S. Hayes, C. Grebogi, Phys. Rev. Lett. 78 (1997) 1247.
[42] E. Bollt, M. Dolnik, Phys. Rev. E 55 (1997) 6404.
[43] F. Bennetto, G. Gallavotti, P.L. Garrido, Chaotic principle: an experimental test, Physica D 105 (4) (1997) 226.
[44] G. Gallavotti, Chaotic principle: some applications to developed turbulence, J. Statist. Phys. 86 (5–6) (1997) 907.